Phonon-mediated drag between one-dimensional electron systems

O. E. Raichev
Institute of Semiconductor Physics, National Academy of Sciences of the Ukraine, Prospekt Nauki 45, Kiev, 03028, Ukraine
(Received 23 January 2001; published 28 June 2001)

The acoustic-phonon-mediated drag between spatially separated one-dimensional electron systems in quantum wires is studied theoretically. The electron transport is assumed to be nearly ballistic. Both deformation- and piezoelectric-potential mechanisms of the electron-phonon interaction are taken into account. It is found that under conditions $2k_Fd \gg 1$, where d is the interwire distance and k_F the Fermi wave number of electrons, the increase of the drag resistance with increasing temperature T evolves from the power-law dependence to the exponential one, and then again to the power-law one. If the product $2k_Fd$ is large enough, the phonon-mediated drag in one-dimensional electron systems becomes more important than the Coulomb drag as the temperature increases. At large T and at $2k_Fd \gg 1$ the phonon-mediated drag resistance is found to be inversely proportional to d.

DOI: 10.1103/PhysRevB.64.035324 PACS number(s): 73.61.−r, 73.50.Dn

I. INTRODUCTION

The mutual friction between spatially separated low-dimensional electron layers gives rise to electron drag phenomenon, which has been attracting a considerable attention in modern condensed matter physics.[1] This phenomenon allows one to investigate electron-electron interaction in low-dimensional systems through the measurements of the transport coefficients. The quantity usually measured in experiments is the drag resistance $R_D = -V_D/I$, where I is the current in one (drive) layer and V_D is the voltage developed in the other (drag) layer, when no current is allowed to flow in the latter. In past years, the studies were focused mostly on the electron drag between two-dimensional (2D) systems.[1] A limited number of theoretical papers[2–12] has been devoted to the drag between one-dimensional (1D) systems. Both Fermi liquid[2–8] and Luttinger liquid[9–12] descriptions of 1D electrons have been employed. Recent experimental observations of electron drag in ballistic quantum wires[13,14] are expected to stimulate further investigations of this phenomenon in 1D systems.

Apart from the direct contribution to the interlayer momentum transfer, caused by the Coulomb interaction (Coulomb drag), there exists an alternate contribution coming from phonon exchange between the layers (phonon-mediated drag). At low temperatures this contribution is determined by the interaction of electrons with acoustic phonons. In spite of weakness of the electron-phonon coupling, the phonon-mediated drag in 2D systems is found to be important, because at large distances between 2D layers it appears to be stronger than the Coulomb drag. The dependence of the phonon-mediated drag on the temperature and parameters of 2D electron layers has been investigated both theoretically[15,17,18] and experimentally.[16,19] In contrast, there were no studies of the phonon-mediated drag between 1D electron systems. The aim of this paper is to investigate the phonon-mediated drag in 1D case under the simplest approximations, when the electron systems in the quantum wires are assumed to be normal Fermi liquids, and the phonon confinement effects are neglected.

The paper is organized as follows. In Sec. II the formalism involved in the calculations is described and the drag resistance is expressed through the integral over the squared module of the matrix element of effective interaction, weighted with a temperature-dependent factor. In Sec. III this matrix element is calculated under the assumption that the distance between the wires is large in comparison to the wire widths. In Sec. IV the analytical expressions for the drag resistance are derived for several temperature regions determined by the characteristic energy scales associated with Fermi wave number, interwire distance, and wire widths. A comparison of the relative contributions of the deformation- and piezoelectric-potential mechanisms of the electron-phonon interaction into phonon-mediated drag, the comparison of the latter with the Coulomb drag, and a brief discussion are given in Sec. V. The Appendix contains expressions of the equilibrium Green's functions of Keldysh's technique for electrons and phonons, which are employed in the calculations in Sec. II.

II. FORMALISM

Consider two homogeneous 1D quantum layers (wires) of length L, labeled 1 and 2, along the axis x. The wires are adiabatically connected to four leads at the ends labeled $+$ and $-$. Each lead is characterized by its own chemical potential $\mu_{j\pm} = \mu + eV_{j\pm}$, $j = 1,2$, where μ is the equilibrium chemical potential. If the tunnel coupling between the layers is neglected, one can write the generalized quantum kinetic equations for each layer using electron Green's functions $G^{\alpha\beta}_{j\varepsilon}$ of Keldysh's technique[20] (here α and β are the standard indices of this technique, $+$ or $-$, and they should not be mixed with the indices of the ends of the wires). In Wigner representation, the equation for layer j is written as

$$v_p^j \frac{\partial}{\partial x} G^{-+}_{j\varepsilon}(p,x) = i\mathcal{I}_{j\varepsilon}(p,x) = -i\Sigma^{-+}_{j\varepsilon}(p,x) G^{+-}_{j\varepsilon}(p,x) + i\Sigma^{+-}_{j\varepsilon}(p,x) G^{-+}_{j\varepsilon}(p,x), \tag{1}$$

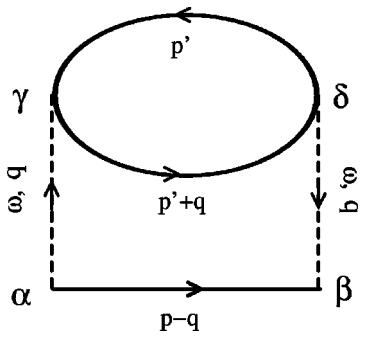

FIG. 1. Diagrammatic representation of the contribution to the electron self-energy due to phonon exchange between the layers.

where p is the electron momentum, v_p^j is the group velocity in the layer j, and $\mathcal{I}$ is the generalized collision integral. Throughout the paper, the system of units where $\hbar=1$ and $k_B=1$ is used. Equation (1) is valid when $pL\gg 1$ and $pl\gg 1$, where l is the mean free path of 1D electrons (note that since in the ballistic regime $l\gg L$, only the first strong inequality is necessary). The self-energy functions $\Sigma_{j\varepsilon}^{\alpha\beta}(p,x)$ describe the interactions. Consider the interaction of electrons with acoustical phonons, which causes a coupling between the electrons in the layers. The lowest-order contribution to $-i\Sigma_{j\varepsilon}^{\alpha\beta}(p,x)$ is represented by the diagram in Fig. 1. The solid and dashed lines, respectively, correspond to $iG_{j\varepsilon}^{\alpha\beta}(p)$ and $iD_{\lambda\omega}^{\alpha\beta}(\mathbf{Q})$, where D is the phonon Green's function. Next, $\mathbf{Q}=(q_x,q_y,q_z)$ is the three-dimensional momentum of the phonon and $\lambda=l,t$ corresponds to longitudinal and transverse polarizations. The vertex in the point $+$ or $-$ corresponds to the matrix element of the Hamiltonian of electron-phonon interaction $V_{\zeta j}(\mathbf{Q})$ multiplied by $+i$ or $-i$, respectively. The index $\zeta=l,t_1,t_2$ numbers the longitudinal and two transverse phonon branches. In the analytical form, the self-energy function drawn in Fig. 1 is

$$\Sigma_{j\varepsilon}^{\alpha\beta}(p)=2\int\frac{d\omega}{2\pi}\int\frac{d\varepsilon'}{2\pi}\sum_{\lambda\lambda'}\sum_{\gamma\delta}l_{\alpha\beta\gamma\delta}\sum_{p'q}\sum_{\mathbf{q}_\perp\mathbf{q}_\perp'}G_{j\varepsilon-\omega}^{\alpha\beta}\times(p-q)G_{j'\varepsilon'}^{\delta\gamma}(p')G_{j'\varepsilon'+\omega}^{\gamma\delta}(p'+q)\times D_{\lambda\omega}^{\alpha\gamma}(\mathbf{Q})D_{\lambda'\omega}^{\delta\beta}(\mathbf{Q}')W_\lambda(\mathbf{Q})W_{\lambda'}(-\mathbf{Q}'),\qquad(2)$$

where $j'\neq j$, $q=q_x$, $\mathbf{q}_\perp=(q_y,q_z)$, $\mathbf{Q}=(q,\mathbf{q}_\perp)$, $\mathbf{Q}'=(q,\mathbf{q}_\perp')$, $W_l(\mathbf{Q})=V_{lj}(\mathbf{Q})V_{lj'}(-\mathbf{Q})$, $W_t(\mathbf{Q})=V_{t_1j}(\mathbf{Q})V_{t_1j'}(-\mathbf{Q})+V_{t_2j}(\mathbf{Q})V_{t_2j'}(-\mathbf{Q})$, and the coordinate index of Green's functions is omitted. The factor $l_{\alpha\beta\gamma\delta}$ is equal to 1 for even number of the indices of one sign and to -1 for odd number of the indices of one sign. The presence of a closed loop of electron lines and spin summation in this loop gives an additional factor of -2 in Eq. (2).

Consider the interaction of electrons with both deformation (microscopic) and piezoelectric (macroscopic) fields generated by the acoustical phonons in the crystals of zinc blend symmetry, assuming that the quantum wires lie in the plane of crystallographic axes and are directed along one of the axes. The matrix elements are given by

$$V_{\zeta j}=\frac{F_j(\mathbf{q}_\perp)}{\sqrt{2\rho\omega_{\lambda\mathbf{Q}}V}}\left[i\mathcal{D}\mathbf{Q}\mathbf{d}_{\zeta\mathbf{Q}}+eh_{14}\beta_{ilk}\frac{Q_iQ_ld_{\zeta\mathbf{Q}}^k}{Q^2}\right],\qquad(3)$$

where $\mathcal{D}$ is the deformation potential constant, eh_{14} is the piezoelectric constant, β_{ilk} is the tensor equal to 1 for $i\neq l\neq k$ and equal to 0 otherwise, $\omega_{\lambda\mathbf{Q}}=s_\lambda Q$ is the phonon frequency ($\lambda=t$ stands for $\zeta=t_1$ and $\zeta=t_2$), and $\mathbf{d}_{\zeta\mathbf{Q}}$ is the unit vector of the crystal lattice displacement. Next,

$$F_j(\mathbf{q}_\perp)=\int dy\int dz|\chi_j(y,z)|^2e^{-iq_yy-iq_zz}\qquad(4)$$

is the overlap integral, where $\chi_j(y,z)$ is the wave function describing confinement of the electrons in the wire j. Since the matrix elements of interaction with deformation and piezoelectric fields generated by a phonon $(\lambda\mathbf{Q})$ are shifted with respect to each other by the phase $\pi/2$, these mechanisms do not interfere, and one has

$$W_\lambda=\frac{F_j(\mathbf{q}_\perp)F_{j'}(-\mathbf{q}_\perp)}{2\rho s_\lambda V}\left[\delta_{\lambda,l}\mathcal{D}^2Q+(eh_{14})^2\frac{A_\lambda}{Q}\right],\qquad(5)$$

where $j\neq j'$, and the anisotropy factors A_λ are given by[21]

$$A_l(\mathbf{Q})=36q_x^2q_y^2q_z^2/Q^6,\qquad A_t(\mathbf{Q})=4(q_x^2q_y^2+q_y^2q_z^2+q_z^2q_x^2)/Q^4-A_l.\qquad(6)$$

In the following, layer 1 is chosen to be the drag layer and layer 2 the drive one. Consider Eq. (1) for $j=1$. It is convenient to introduce[22] the energy distribution functions for the electrons with the positive group velocity (moving from $+$ to $-$) and with the negative one (moving from $-$ to $+$), according to

$$g_{1\varepsilon}^{\pm}(x)=\pm\int_0^{\pm\infty}\frac{dp}{2\pi i}|v_p|G_{1\varepsilon}^{-+}(p,x).\qquad(7)$$

With use of Eq. (7), Eq. (1) is transformed to a pair of equations for g^+ and g^-:

$$\pm\frac{\partial}{\partial x}g_{1\varepsilon}^{\pm}(x)=I_{1\varepsilon}^{\pm}(x),\qquad(8)$$

where the functions $I_{1\varepsilon}^{\pm}$ are defined as $I_{1\varepsilon}^{\pm}(x)=\pm(2\pi)^{-1}\int_0^{\pm\infty}dp\mathcal{I}_{1\varepsilon}(p,x)$. The boundary conditions for Eq. (8) at $x=0$ and $x=L$ are determined by the chemical potentials of the leads to which the drag wire is connected:

$$g_{1\varepsilon}^{+}(0)=[e^{(\varepsilon-\mu_{1+})/T}+1]^{-1},\qquad g_{1\varepsilon}^{-}(L)=[e^{(\varepsilon-\mu_{1-})/T}+1]^{-1}.\qquad(9)$$

The general expression for the electric current in the layer j is

$$J_j=2e\int\frac{d\varepsilon}{2\pi i}\int\frac{dp}{2\pi}v_p^jG_{j\varepsilon}^{-+}(p,x).\qquad(10)$$

Using Eqs. (7)–(10), one obtains

$$J_1=\frac{e}{\pi}\int d\varepsilon[g^+_{1\varepsilon}(x)-g^-_{1\varepsilon}(x)]$$

$$=G_0(V_{1+}-V_{1-})+\frac{G_0}{e}\int_0^L dx\int d\varepsilon I^+_{1\varepsilon}(x), \qquad (11)$$

where $G_0=e^2/\pi$ is the conductance quantum. In the experiments one measures the drag voltage $V_D=V_{1+}-V_{1-}$ at $J_1=0$. Thus, Eq. (11) can be used for determination of V_D through the drive voltage $V=V_{2+}-V_{2-}$.

The function $I^+_{1\varepsilon}(x)$ in Eq. (11) depends on both V and V_D. However, if the drag effect is weak, i.e., $|V_D|$ is much less than $|V|$, one can substitute the equilibrium Green's functions $G^{(0)\alpha\beta}_{1\varepsilon}(p)$ (see the Appendix) instead of $G^{\alpha\beta}_{1\varepsilon}(p)$ into $I^+_{1\varepsilon}(x)$. Using also the equilibrium Green's functions of the free phonons (see the Appendix) in Eq. (2), after some transformations one gets

$$I^+_{1\varepsilon}=2\int_0^\infty\frac{dp}{2\pi}\int d\omega\int d\varepsilon'\int\frac{dp'}{2\pi}\int\frac{dq}{2\pi}|M(\omega,q)|^2$$
$$\times G^c_{1,\varepsilon}(p)G^c_{1,\varepsilon-\omega}(p-q)\{f(\varepsilon-\omega)$$
$$\times[1-f(\varepsilon)]G^{+-}_{2,\varepsilon'}(p')G^{-+}_{2,\varepsilon'+\omega}(p'+q)-f(\varepsilon)$$
$$\times[1-f(\varepsilon-\omega)]G^{-+}_{2,\varepsilon'}(p')G^{+-}_{2,\varepsilon'+\omega}(p'+q)\}, \qquad (12)$$

where

$$M(\omega,q)=L\sum_{\lambda\mathbf{q}_\perp}\frac{2\omega_{\lambda\mathbf{Q}}}{\omega^2-\omega^2_{\lambda\mathbf{Q}}+i0}W_\lambda(\mathbf{Q}). \qquad (13)$$

The term $M(\omega,q)$ contains all information about the phonons. It comprises both real and virtual phonon contributions and is called the matrix element of effective interaction.

Taking into account that the transport in the drive wire is ballistic, one can replace $G^{-+}_{2\varepsilon}(p)$ by the quasiequilibrium Green's function $2\pi i G^c_{2\varepsilon}(p)f_{2p}(\varepsilon)$, where the energy distribution is dictated by the leads $f_{2p}(\varepsilon)=f(\varepsilon-eV_{2+})$ for $p>0$ and $f_{2p}(\varepsilon)=f(\varepsilon-eV_{2-})$ for $p<0$. The collision integral (12) is nonzero only if the signs of p' and $p'+q$ are opposite, i.e., when the backscattering takes place in the drive wire. Substituting I^+ from Eq. (12) to Eq. (11) and assuming the linear transport regime, $eV\ll T$, one finds

$$J_1=G_0V_D+V\frac{e^2L}{\pi^2T}\int_0^\infty dp\int_{-\infty}^0 dp'\int_{-p'}^\infty dq\int d\omega\int d\varepsilon$$
$$\times\int d\varepsilon'|M(\omega,q)|^2G^c_{1,\varepsilon}(p)G^c_{1,\varepsilon-\omega}(p-q)G^c_{2,\varepsilon'}(p')$$
$$\times G^c_{2,\varepsilon'+\omega}(p'+q)f(\varepsilon)[1-f(\varepsilon-\omega)]f(\varepsilon')$$
$$\times[1-f(\varepsilon'+\omega)]. \qquad (14)$$

Equation (14) provides an explicit relation between the drag voltage V_D and the drive voltage V at $J_1=0$. In the following, the free-electron approximation is used, when $G^c_{j\varepsilon}(p)=\delta(\varepsilon-\varepsilon_{jp})$. Assuming that the electrons in the wires are described by parabolic dispersion laws $\varepsilon_{1p}=\Delta/2+p^2/2m$ and $\varepsilon_{2p}=-\Delta/2+p^2/2m$, shifted with respect to each other by the energy Δ, one can easily calculate the integrals over ε, ε', p, and p'. As a result,

$$\frac{V_D}{V}=-\frac{Lm^2}{4\pi T}\int_{-\infty}^\infty d\omega\int_{\sqrt{m\omega}}^\infty dq\frac{|M(\omega,q)|^2}{q^2P^+_{\omega q}P^-_{\omega q}},$$

$$P^\pm_{\omega q}=\cosh\gamma_{\omega q}+\cosh[(\omega\pm\Delta)/2T], \qquad (15)$$

$$\gamma_{\omega q}=\omega^2m/2q^2T+q^2/8mT-\mu/T.$$

The denominator $P^+_{\omega q}P^-_{\omega q}$ rapidly increases when either ω or Δ exceeds $2T$, and the expression under the integrals has a sharp maximum, as a function of q, around $q=q_m$ satisfying $\gamma_{\omega q_m}=0$. Since ω is much smaller than the Fermi energy, one can find that $q_m\simeq 2k_F$, where the Fermi wave number k_F is equal to $\sqrt{2m\mu}$. Assuming that $|M(\omega,q)|^2$ slowly changes in the region $\delta q\sim 2mT/k_F$ around $q=2k_F$, it is possible to replace $M(\omega,q)$ in Eq. (15) by $M(\omega,2k_F)$ and take the integral over q, expanding $\gamma_{\omega q}$ near q_m as $\gamma_{\omega q}=q_m(q-q_m)/4mT$. A justification of this assumption is the following. In the next section, it is shown that $|M(\omega,q)|^2$ changes with q on the scales $q\sim 1/d$ and $q\sim\omega/s_\lambda$. Therefore, the substitution $q=2k_F$ is justified as long as $T\ll k_F/md$ and $T\ll k_F\omega/ms_\lambda$. The first of these conditions is easy to fulfill at low enough temperatures. As for the second one, the characteristic frequency ω is estimated as either T or $s_\lambda q$, so that it is valid when the Fermi velocity is great in comparison to the sound velocities and the Fermi energy is great in comparison to the temperature. Both these requirements are assumed.

The drag resistance $R_D=-V_D/J_2=-(V_D/V)G_0^{-1}$ is finally expressed as

$$R_D=\frac{L}{2v_F^3e^2}\int_0^\infty d\omega|M(\omega,2k_F)|^2\Phi_{\Delta/2T}(\omega/2T), \qquad (16)$$

$$\Phi_\nu(x)=\frac{x\coth x-\nu\coth\nu}{\cosh^2x-\cosh^2\nu}.$$

This expression formally coincides with the one obtained for Coulomb drag[6,7] if $|M(\omega,2k_F)|^2$ is replaced by the frequency-independent squared interlayer Coulomb matrix element $|M(2k_F)|^2\simeq(2e^2/\epsilon)^2K_0^2(2k_Fd)$, where ϵ is the static dielectric constant and K_0 is the modified Bessel function; the remaining integral $\int_0^\infty\Phi_{\Delta/2T}(\omega/2T)d\omega$ is equal to $(\Delta^2/4T)/\sinh^2(\Delta/2T)$, producing a simple temperature dependence $R_D\sim T$ at $\Delta\to 0$. In contrast, for the phonon-mediated drag the frequency dependence of the effective interaction $M(\omega,2k_F)$ is essential. For this reason, both temperature and interlayer separation behavior of the phonon-mediated drag appear to be more complicated than of the Coulomb drag. To determine them, it is necessary to calculate the effective interaction. This is the subject of the next section.

III. THE EFFECTIVE INTERACTION

The effective interaction is described by Eqs. (13) and (4)–(6). The calculation of the overlap integrals $F_j(\mathbf{q}_\perp)$ in this section is based upon the model of quantum wires in planar coupling geometry.[23,13] Such wires are obtained from a 2D electron layer formed at the heterojunction interface (perpendicular to z axis) by the electrostatic depletion in y direction. With a good accuracy, the wave functions $\chi_j(y,z)$ can be modelled by properly normalized products of the Fang-Howard wave function $ze^{-z/2b}$ by the Gaussian functions $e^{-(y-y_j)^2/2a^2}$. The wires are assumed to be identical and interwire distance d is expressed as $d=|y_1-y_2|$. Then, a calculation of the overlap integral gives

$$\mathrm{Re}\,F_1(\mathbf{q}_\perp)F_2(-\mathbf{q}_\perp)=\frac{e^{-a^2q_y^2/2}\cos q_y d}{(1+q_z^2b^2)^3}, \tag{17}$$

while $\mathrm{Im}\,F_1(\mathbf{q}_\perp)F_2(-\mathbf{q}_\perp)$ is an odd function of q_y, which does not contribute into $M(\omega,q)$. Other models of double quantum wires, such as the wires of vertical coupling geometry,[24,25] can be considered as well. The lengths a and b are the characteristic widths of the wires, in y and in z directions, respectively.

The effective interaction $M(\omega,q)$ is represented as a sum of two terms $M_\lambda(\omega,q)$:

$$M_\lambda(\omega,q)=-\frac{1}{\rho s_\lambda^2}\int_{-\infty}^{\infty}\frac{dq_y}{2\pi}Y_\lambda(\omega,q,q_y)e^{-a^2q_y^2/2}\cos q_y d, \tag{18}$$

where the integrals

$$Y_\lambda=\int_{-\infty}^{\infty}\frac{dq_z}{2\pi}\frac{\mathcal{D}^2Q^2\delta_{\lambda,l}+(eh_{14})^2A_\lambda(\mathbf{Q})}{(1+q_z^2b^2)^3[Q^2-\omega^2/s_\lambda^2-i0]} \tag{19}$$

can be calculated exactly. However, the exact expressions are rather complicated. The approximate result, corresponding to small b, is given below:

$$Y_l\simeq\mathcal{D}^2\left[\frac{3}{16b}+\frac{\omega^2}{2s_l^2q_l}\right]-(eh_{14})^2q^2\left[18\frac{s_l^6}{\omega^6}(q_l^3-q^2q_l-q_1^3+q^2q_1)+9\frac{s_l^4}{\omega^4}(2q_l+q_1-q^2/q_1)+\frac{9s_l^2}{4\omega^2}(1/q_1-q^2/q_1^3)\right] \tag{20}$$

and

$$Y_t\simeq(eh_{14})^2\left[18\frac{s_t^6}{\omega^6}q^2(q_t^3-q^2q_t-q_1^3+q^2q_1)+\frac{s_t^4}{\omega^4}(-2q_t^3+20q^2q_t-2q^4/q_t+2q_1^3+7q^2q_1-7q^4/q_1)+\frac{s_t^2}{\omega^2}[-2q_t+2q^2/q_t-q_1+(5/4)q^2/q_1-(5/4)q^4/q_1^3]\right], \tag{21}$$

where

$$q_1=(q^2+q_y^2)^{1/2},\qquad q_\lambda=(q^2+q_y^2-\omega^2/s_\lambda^2-i0)^{1/2}. \tag{22}$$

This result is applicable under the following conditions:

$$(q^2+q_y^2)b^2\ll1,\quad(\omega b/s_\lambda)^2\ll1. \tag{23}$$

The reliability of these conditions can be checked as follows. Since the characteristic q_y contributing in the integral in Eq. (18) are not great in comparison to either $q\simeq2k_F$ or ω/s_λ, the first condition can be replaced by $(2k_Fb)^2\ll1$. The width b is given[26] by $b=(33\pi N_{2D}/2a_B)^{-1/3}$, where $a_B=\epsilon/me^2$ is the Bohr radius and N_{2D} is the sheet electron density on the interface. For GaAs-based structures ($\epsilon\simeq13$) at typical density $N_{2D}\simeq2\times10^{11}$ cm^{-2} used in experiments, b is less than 5 nm. On the other hand, the maximal Fermi wave number in the quantum wire, in conditions when only one 1D subband is populated, is of the order of a^{-1}. Typical values of a are from 20 to 30 nm, so that $a^2\gg b^2$. This strong inequality reflects the fact that the lateral confinement energy (which is usually a few meV) is much smaller than the energy of quantization in z direction (which is of the order of 100 meV). Thus, $(2k_Fb)^2\ll1$ is fulfilled. As for the second condition, it requires rather small temperatures, since the characteristic ω contributing into the integral in Eq. (16) cannot be much larger than T. The ballistic transport regime is normally realized at $T<1$ K. Then, using $b\simeq5$ nm, and sound velocities in GaAs (see below), one can find that $(s_\lambda/bT)^2\gg1$ at such small temperatures. Therefore, the second condition of Eq. (23) is also valid under reasonable assumptions.

The calculation is continued below in the limit $d\gg a$, which is consistent with present experimental situation for double quantum wire systems of planar geometry,[13,14] where $d\simeq200$ nm. Neglecting the terms proportional to $e^{-d^2/2a^2}$, it is possible to calculate the integral over q_y in Eq. (18) analytically, which gives

$$\begin{aligned}M_l(\omega,q)=&-\frac{(eh_{14})^2e^{a^2q^2/2}}{\pi\rho s_l^2}\{9(u^4-u^2/4)K_0(qd)\\&+[(18u^6+9u^4)/qd+9u^2qd/4]K_1(qd)\\&+54u^6K_2(qd)/(qd)^2-e^{-a^2\omega^2/2s_l^2}\\&\times[18u^3(u^2-1)^{3/2}K_1(\kappa_ld)/qd\\&+54u^4(u^2-1)K_2(\kappa_ld)/(qd)^2]\}\\&-\frac{\mathcal{D}^2\omega^2}{2\pi\rho s_l^4}e^{a^2q^2/2-a^2\omega^2/2s_l^2}K_0(\kappa_ld)\\\equiv&M_l^P+M^D,\end{aligned} \tag{24}$$

where $u=s_lq/\omega$, and

$$M_t(\omega,q)=-\frac{(eh_{14})^2e^{a^2q^2/2}}{\pi\rho s_t^2}\{(-7v^4+5v^2/4)K_0(qd)$$
$$+[(v^2-7v^4-18v^6)/qd-5v^2qd/4]K_1(qd)$$
$$+6v^4(1-9v^2)K_2(qd)/(qd)^2-e^{-a^2\omega^2/2s_t^2}$$
$$\times[2v^2(v^2-1)K_0(\kappa_t d)+2v(v^2-1)^{3/2}$$
$$\times(1-9v^2)K_1(\kappa_t d)/qd+6v^2(v^2-1)$$
$$\times(1-9v^2)K_2(\kappa_t d)/(qd)^2,]\}$$
$$\equiv M_t^P, \tag{25}$$

where $v=s_tq/\omega$. In Eqs. (24) and (25) $\kappa_\lambda=(q^2-\omega^2/s_\lambda^2)^{1/2}$ is the complex wave number. If $\omega>s_\lambda q$, then κ_λ and $K_n(\kappa_\lambda d)$ are transformed according to the rule

$$(q^2-\omega^2/s_\lambda^2)^{1/2}\rightarrow -i(\omega^2/s_\lambda^2-q^2)^{1/2},$$
$$K_n(-ix)\rightarrow i^{n+1}(\pi/2)H_n^{(1)}(x), \tag{26}$$

where $H_n^{(1)}(x)$ is the Hankel function.[27] It is expressed through the ordinary Bessel functions of the first and second kind as $H_n^{(1)}(x)=J_n(x)+iN_n(x)$. The rule (26) follows from the fact that ω^2 contains an infinitely small imaginary part, see Eqs. (19) and (22), which is omitted in Eqs. (24) and (25). M_λ are real at $\omega<s_\lambda q$ and complex at $\omega>s_\lambda q$. If ω is much smaller than both $\overline{s}k_F$ and $\overline{s}/d$ (here $\overline{s}$ is the averaged sound velocity), one can expand $K_n(\kappa_\lambda d)$ in power series of ω, which gives

$$M_l(\omega,q)\simeq-\frac{3(eh_{14})^2e^{a^2q^2/2}}{8\pi\rho s_l^2}[qdK_1(qd)-(qd)^2K_0(qd)]$$
$$-\frac{\mathcal{D}^2\omega^2}{2\pi\rho s_l^4}e^{a^2q^2/2}K_0(qd), \tag{27}$$

and

$$M_t(\omega,q)\simeq-\frac{(eh_{14})^2e^{a^2q^2/2}}{8\pi\rho s_t^2}[-qdK_1(qd)$$
$$+(2+(qd)^2)K_0(qd)]. \tag{28}$$

With the increase of ω, the deformation-potential contribution M^D increases and has a logarithmic divergency at $\omega=s_lq$. The piezoelectric-potential contributions M_l^P and M_t^P, are regular at $\omega=s_{l,t}q$. If $qd\gg1$, both M_l and M_t at $\omega>s_{l,t}q$ are great in comparison to M_l and M_t at $\omega\ll s_{l,t}q$. The dependence of the absolute values of the piezoelectric contributions $M_\lambda^P(\omega,q)$ on $\omega/s_\lambda q$, for $qd=1$ and $qd=8$, is shown in Fig. 2. In Fig. 3 the total squared matrix element $|M(\omega,q)|^2$ is shown as a function of ω/s_lq. The material parameters of GaAs used in this calculation are $s_l=5.14\times10^5$ cm/s, $s_l=3.04\times10^5$ cm/s, $\rho=5.31$ g/cm^3, $h_{14}=1.2\times10^7$ V/cm,[21,17] and $\mathcal{D}=10$ eV,[28] and the interlayer distance d is set to 200 nm.

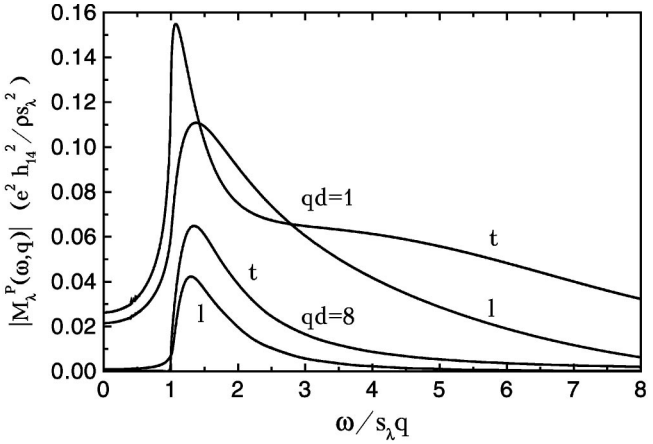

FIG. 2. Frequency dependence of piezoelectric-potential contribution to the effective interaction at $qd=1$ and $qd=8$ ($q^2a^2\ll1$ is assumed). The absolute values of the functions M_l^P and M_t^P, given by Eqs. (24) and (25), are expressed in units of $(eh_{14})^2/\rho s_l^2$ and $(eh_{14})^2/\rho s_t^2$, respectively.

It is important to notice that $|M(\omega,q)|^2$ does not contain any divergency that would make the drag resistance infinite (the logarithmic divergency at $\omega=s_lq$, of course, does not create any problems). In contrast, the theory of phonon-mediated drag in 2D systems encounters the problem of divergency,[17] which can be removed, for example, by introduction of a finite free path for the phonons; this leads to logarithmically large factors in the drag resistance. Mathematically, the difference between the matrix elements of effective interaction in 1D and 2D cases exists because in 2D case the calculation of the matrix element involves a single integral over transverse wave number of the phonon, while in 1D case one has a double integral, over q_z and q_y, which kills the dangerous divergency. From the physical point of view, the reduction of dimensionality from 2D to 1D reduces the number of the phonons participating in the interlayer exchange, thereby making the phonon-mediated drag less effective.

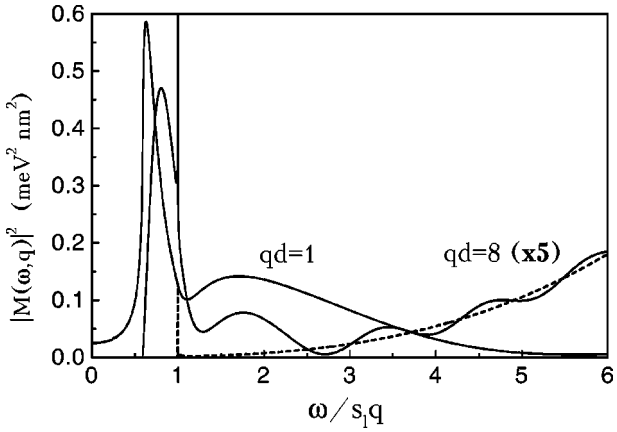

FIG. 3. The squared absolute value of the effective interaction $|M(\omega,q)|^2$ for GaAs wires at $d=200$ nm, $q^2a^2\ll1$, $qd=1$, and $qd=8$. The dashed line shows the deformation-potential contribution $|M^D(\omega,q)|^2$ for $qd=8$ (this contribution is negligible for $qd=1$ in the frequency interval considered). The data for $qd=8$ is multiplied by the factor of 5.

IV. DRAG RESISTANCE

The results obtained in the previous section are used below to evaluate the integral over ω in Eq. (16). For the sake of simplicity, only the case of aligned 1D subbands, $\Delta=0$, is studied. Consider first the region of *low temperatures* $T \ll \overline{s}k_F, \overline{s}/d$. The contribution to the integral comes from small ω, where the approximate expressions (27) and (28) are valid. This gives the polynomial power-law temperature dependence of the drag resistance

$$R_D=\frac{Le^{-4a^2k_F^2}}{e^2\rho^2v_F^3s_l^4}\left[\mathcal{D}^4\frac{\pi^2K_0^2(2k_Fd)}{5s_l^4}T^5 + \mathcal{D}^2(eh_{14})^2\frac{K_0(2k_Fd)B(2k_Fd)}{24s_l^2}T^3 + (eh_{14})^4\frac{B^2(2k_Fd)}{128\pi^2}T\right], \quad (29)$$

where the dimensionless function $B(2k_Fd)$ is given by

$$B(x)=[(x^2+2)r^2-3x^2]K_0(x)+(3-r^2)xK_1(x) \quad (30)$$

and $r=s_l/s_t$ is the sound velocity ratio.

If $2k_Fd\gg1$, the drag resistance at $T\ll2\overline{s}k_F$ can be represented as a sum of two parts

$$R_D=R_D^{(1)}+R_D^{(2)}. \quad (31)$$

The first part is the contribution from the region of small ω. If the characteristic frequencies $\omega\sim2T$ are small in comparison to $2\overline{s}\sqrt{k_F/d}$, this contribution is given by Eq. (29) in the limit $2k_Fd\gg1$:

$$R_D^{(1)}=\frac{\pi Le^{-4k_Fd+4a^2k_F^2}}{4e^2\rho^2v_F^3s_l^4k_Fd}\left[\mathcal{D}^4\frac{\pi^2T^5}{5s_l^4} + (r^2-3)\mathcal{D}^2(eh_{14})^2\frac{(k_Fd)^2T^3}{6s_l^2} + (r^2-3)^2(eh_{14})^4\frac{(k_Fd)^4T}{8\pi^2}\right]. \quad (32)$$

This part is exponentially small, since it is proportional to e^{-4k_Fd}. The second part $R_D^{(2)}$, which rapidly increases with the increasing temperature, is the contribution from the regions of ω just above $\omega_l=2s_lk_F$ and $\omega_t=2s_tk_F$, for the longitudinal and transverse phonons, respectively. Because of the substantial difference between the velocities s_l and s_t, the longitudinal-phonon and transverse-phonon terms in this contribution have to be considered independently. Expanding κ_λ near ω_λ as $\kappa_\lambda=-i2(k_F/s_\lambda)^{1/2}(\omega-\omega_\lambda)^{1/2}$, one finds that the argument of the Bessel functions, $\kappa_\lambda d$, is large at $(\omega-\omega_\lambda)\sim T$, if $T\gg\overline{s}/k_Fd^2$. Therefore, one may use the asymptotic of the Bessel functions at large arguments in calculation of the integrals containing $K_n(\kappa_\lambda d)$. Keeping in Eqs. (24) and (25) only the leading terms with respect to the small parameter $(qd)^{-1}=(2k_Fd)^{-1}$, one can see that piezoelectric-potential contribution is much less important in the longitudinal-phonon terms than in the transverse ones, and, therefore, should be accounted in the transverse terms only. The contribution $R_D^{(2)}$ is represented as a sum of two thermal-activated parts

$$R_D^{(2)}=\frac{L}{\sqrt{2\pi}e^2\rho^2v_F^3d}\left[\frac{2\mathcal{D}^4k_F^4}{s_l^3}\left(\frac{2s_lk_F}{T}\right)^{1/2}e^{-2s_lk_F/T} + \frac{6(eh_{14})^4}{s_t^3}\left(\frac{T}{2s_tk_F}\right)^{3/2}e^{-2s_tk_F/T}\right]. \quad (33)$$

This contribution exponentially increases with temperature, and it does not contain a small factor of e^{-4k_Fd}. From a comparison of the exponents $e^{-2s_tk_F/T}$ and e^{-4k_Fd}, it follows that $R_D^{(2)}$ becomes comparable to $R_D^{(1)}$ as the temperature reaches $s_t/2d$. With the further increase of the temperature, $R_D^{(2)}$ rapidly overcomes $R_D^{(1)}$. The region where the temperature dependence of the drag resistance follows the exponential law (33), can be called as the region of *intermediate temperatures*. This region exists only if $2k_Fd\gg1$. In view of large interwire separation d in existing double-wire devices, this condition is easy to satisfy even at relatively small Fermi energies of 1D electrons. On the other hand, the opposite condition $2k_Fd\ll1$ assumes very small Fermi energies, when it is practically impossible to avoid localization of the electrons due to the inhomogeneities of the wires. For this reason, the case of small $2k_Fd$ is not considered in this paper.

The derivation of Eq. (33) is done under conditions $(qd)^2\gg1$ and $2s_tk_F/T\gg1$. However, because of the large numerical coefficients and large powers of ω/s_tq standing in Eq. (25) for $M_t(\omega,q)$, the expression for the pre-exponential factor in the second term of Eq. (33) is not quite reliable even if qd and $2s_tk_F/T$ are as large as 10, and has to be improved. With more accuracy, the factor $(T/2s_tk_F)^{3/2}$ in this term should be replaced by another temperature-dependent factor

$$[1+7/(qd)^2]I_7(2s_tk_F/T)-63I_9(2s_tk_F/T)/(qd)^2,$$

where the integrals

$$I_k(x)=\frac{4}{3\sqrt{\pi}}x\int_0^\infty dt\frac{t^{3/2}e^{-xt}}{(1+t)^k}$$

are not reduced to $x^{-3/2}$ at $x\gg1$ if k is large.

Consider now the region of relatively *high temperatures*, when $T\gg\overline{s}k_F$, and the contribution in the integral in Eq. (16) comes from large frequencies. Under conditions $k_Fa\ll1$ one can notice a qualitative difference in behavior of the piezoelectric-potential and the deformation-potential parts of $M(\omega,2k_F)$ at $\omega>\overline{s}k_F$. The former, $M^P=M_l^P+M_t^P$, decreases with ω on the scale $\omega\sim\overline{s}k_F$, and the contribution to the integral over ω in Eq. (16) coming from $|M^P(\omega,2k_F)|^2$ converges on this scale. The latter, M^D, increases with ω, and the contribution to the integral in Eq. (16) coming from $|M^D(\omega,2k_F)|^2$ converges either at $\omega\sim2T$ or at $\omega\sim s_l/a$: in

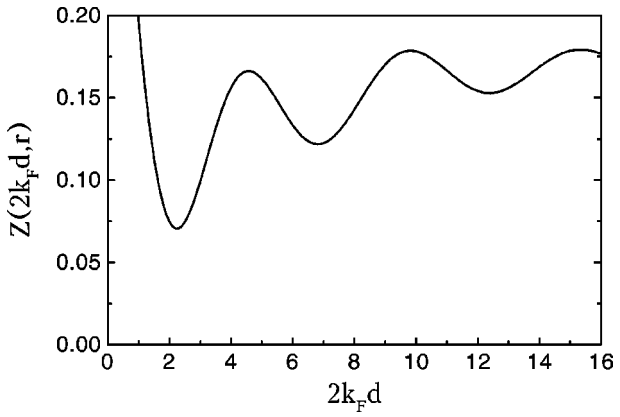

FIG. 4. The function $Z(2k_Fd,r)$, entering Eq. (35), at $r=1.69$.

any case $\omega \gg \overline{sk}_F$. The drag resistance associated with both parts considered above can be represented as a sum of two terms

$$R_D = R_D^P + R_D^D, \tag{34}$$

and the cross-term contribution, caused by the interference of piezoelectric-potential and deformation-potential parts, is neglected. It is always small in comparison to either R_D^D or R_D^P, because the regions of ω contributing to R_D^P and R_D^D are essentially different.

The term R_D^P is proportional to the integral $\int d\omega |M^P(\omega,2k_F)|^2 \Phi_0(\omega/2T)$, which converges at $\omega \sim 2\overline{sk}_F$. Therefore, the terms $e^{-a^2\omega^2/2s_\lambda^2}$ in M^P should be replaced by 1, and $\Phi_0(\omega/2T)$ should be replaced by $\Phi_0(0) = 1/3$. This term describes temperature-independent contribution to the drag resistance

$$R_D^P = \frac{L(eh_{14})^4 Z(2k_Fd,r)}{6e^2\rho^2 v_F^3 s_l^3 d}, \tag{35}$$

where Z is a dimensionless function plotted in Fig. 4 for $r = 1.69$, the ratio of sound velocities in GaAs. The oscillations of this function appear because of the interference of different oscillating terms from M_l^P and M_t^P at $\omega > 2s_lk_F$ and $\omega > 2s_tk_F$, see Eqs. (24) and (25). As k_Fd increases, the oscillations weaken and $Z(2k_Fd,r)$ saturates to the value of $4r^3/35\pi \simeq 0.176$.

Since the characteristic frequencies contributing to $R_D^D \sim \int d\omega |M^D(\omega,2k_F)|^2 \Phi_0(\omega/2T)$ are much larger than $\overline{sk}_F$, it is possible to use the asymptotic of the Bessel function $K_0(\kappa_l d)$ at large arguments in calculation of the integral. This part is given by

$$R_D^D = \frac{L\mathcal{D}^4 T^4 \Lambda(2Ta/s_l)}{\pi e^2 \rho^2 v_F^3 s_l^7 d}, \tag{36}$$

where

$$\Lambda(x) = \int_0^\infty dt\, t^3 \Phi_0(t) e^{-x^2t^2} \tag{37}$$

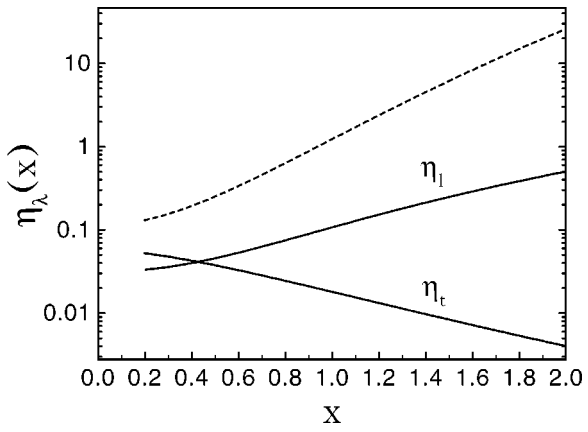

FIG. 5. Solid lines: functions $\eta_l(x)$ and $\eta_t(x)$, defined by Eqs. (39) and (40). Dashed line: the ratio of $\eta_l(x)/r^3\eta_t(x)$ at $r=1.69$.

if $T \ll s_l/a$, $\Lambda(2Ta/s_l) = 3\zeta(3)/2 \simeq 1.803$. In this case R_D^D increases with the temperature as T^4. In the opposite limit the temperature dependence vanishes.

Consider now the case $k_Fa \sim 1$. This also implies $2k_Fd \gg 1$, and only the leading-order terms with respect to this parameter should be kept in $|M(\omega,q)|^2$. Both the polarization-potential and deformation-potential contributions to the integral in Eq. (16) converge at $\omega \sim \overline{s/a}$, since under the conditions $T \gg \overline{sk}_F$ one has also $T \gg \overline{s/a}$, and $\Phi_0(\omega/2T)$ should be replaced by 1/3. This means that the drag resistance is temperature-independent. It is given by

$$R_D = \frac{L}{3\pi e^2 \rho^2 v_F^3 s_l^3 d}[(eh_{14})^4 r^3 \eta_t(2k_Fa) + (\mathcal{D}/a)^4 \eta_l(2k_Fa)], \tag{38}$$

where

$$\eta_l(x) = \left(\frac{x}{2}\right)^4 \int_1^\infty dt \frac{t^4 e^{x^2(1-t^2)}}{\sqrt{t^2-1}}, \tag{39}$$

and

$$\eta_t(x) = \int_1^\infty dt\, t^{-8}(t^2-1)^{3/2} e^{x^2(1-t^2)}. \tag{40}$$

The cross-term contribution to R_D is neglected in Eq. (38). It is small because of the presence of the fast-oscillating factor $\cos[d\sqrt{\omega^2/s_t^2 - 4k_F^2} - d\sqrt{\omega^2/s_l^2 - 4k_F^2}]$ under the integral over ω for this contribution. The functions $\eta_l(x)$ and $\eta_t(x)$, as well as the ratio of $\eta_l(x)/r^3\eta_t(x)$ at $r=1.69$ are shown in Fig. 5.

Equations (35), (36), and (38) show that in the region of high temperatures $T \gg \overline{sk}_F$ the drag resistance is inversely proportional to the interwire separation d [at $k_Fa \ll 1$ this is true under conditions $2k_Fd \gg 1$, when $Z(2k_Fd,r)$ is constant]. The same dependence, at $2k_Fd \gg 1$, takes place in the region of intermediate temperatures, see Eq. (33). The law $R_D \propto 1/d$ has a simple physical explanation. If $2k_Fd \gg 1$ and the temperature is large enough, the main contribution to the

integral of Eq. (16) comes from the frequencies $\omega > 2s_\lambda k_F$. This is the region of *real* phonon exchange. Thus, at $d \gg a$ the drive wire can be roughly considered as a line emitting phonons, while the drag wire is a line receiving phonons, and the drag rate is proportional to the intensity of the radiation received. In this model, the spatial distribution of the phonons emitted have cylindrical symmetry, so that the intensity of the radiation decreases with the distance d between the wires as $1/d$, and so does the drag resistance. A similar consideration shows that the phonon-mediated drag between 2D layers does not depend on the interlayer separation d at large enough T and d. Of course, if one accounts for finite lifetime of the phonons, the drag resistance should decrease with d faster.

V. DISCUSSION

In this paper, a theoretical study of the phonon-mediated drag between the electrons in two parallel one-dimensional conductors (quantum wires) has been done. The electron systems have been assumed to be normal Fermi liquids. The electron transport has been assumed to be nearly ballistic, which means that most of the electrons pass through the wires without any scattering. The phonons have been described within the bulk mode (three-dimensional) approximation, which is reliable if the difference between the densities, elastic modules and piezomodules of the crystals forming the heterostructure is not substantial. Both the deformation-potential and piezoelectric-potential interaction between the electrons and phonons have been considered. The detailed calculations of the matrix element of effective interaction and of the drag resistance R_D have been done for the case when the interwire separation d is large in comparison to the characteristic width a of the electron systems determined by the lateral confinement in the wires.

The temperature, electron density, and interlayer separation dependencies of the phonon-mediated drag are rather complicated. Though the drag resistance always increases with the temperature, one should stress that in the different regions of T, which are determined by the characteristic energy scales $\bar{s}/d$, $\bar{s}/a$, and $\bar{s}k_F$, the temperature dependence of R_D is considerably different. If $2k_F d \gg 1$, there exists a region of intermediate temperatures, characterized by exponential increase of R_D with T. This region separates the low-temperature ($T \ll \bar{s}/d$) and high-temperature ($T \gg \bar{s}k_F$) regions, where the temperature dependencies are given by different polynomial power laws. In the low-temperature region, when the drag is dominated by virtual phonon exchange, R_D is proportional to $e^{-4k_F d}$, while at higher temperatures, when the drag is dominated by real phonon exchange, R_D is proportional to $1/d$.

The results obtained allow to compare relative contributions of the piezoelectric- and deformation-potential mechanisms of the phonon-mediated drag in the quantum wires. It is very important also to compare the phonon-mediated drag contribution with Coulomb drag contribution in such systems. Both these tasks are done below with use of the material parameters of GaAs.

Taking the values of eh_{14} and $\mathcal{D}$ given in the end of Sec. III, one can estimate the ratio $\mathcal{D}/eh_{14}$ in GaAs as 8.3 nm. An analysis of Eqs. (29)–(33) under condition shows that the piezoelectric-potential contribution dominates in the region $T \ll \bar{s}k_F$. In the high-temperature region $T \gg \bar{s}k_F$ and at $k_F a \ll 1$, one should compare Eqs. (35) and (36), taking into account that $Z \sim 0.1$ (see Fig. 4). This again shows that the piezoelectric-potential contribution dominates. Only when $T \gg \bar{s}k_F$ and $k_F a \sim 1$, both contributions can be comparable, as follows from the analysis of Eq. (38), see Fig. 5. This temperature region, however, lies well above 1 K, where the ballistic transport regime in quantum wires is hardly achievable. Therefore, one should consider the piezoelectric-potential mechanism of electron-phonon interaction as the main cause of the phonon-mediated drag in GaAs quantum wires. Still, the deformation-potential mechanism can become comparable with the piezoelectric-potential one even at $T < 1$ K in the quantum wires fabricated from a different material, where the ratio $\mathcal{D}/eh_{14}$ is greater [note that the comparison is based upon the factor of $(\mathcal{D}/eh_{14})^4$]. An example of such a material is InAs, where the piezoelectric constant is about four times smaller than in GaAs.

Within the same approximations as used in the calculations above, the Coulomb drag is given by a simple formula[6,7]

$$R_D^C = \frac{2LTe^2}{\epsilon^2 v_F^3}\left[\frac{1}{\pi a^2}\int dy \int dy' e^{-y^2/a^2-(y'+d)^2/a^2} \times K_0(2k_F|y-y'|)\right]^2. \tag{41}$$

The factor $[\cdots]^2$ in this equation can be approximated by $K_0^2(2k_F d)$, with a good accuracy. This approximation is used below in comparison of R_D^C with R_D, the latter is calculated in the previous sections. Only the piezoelectric-potential contribution to R_D is taken into account, as the main one. It is interesting that in the region $T \ll \bar{s}/d$ both R_D and R_D^C are described by the functions proportional to $Te^{-4k_F d}$, and a comparison of them shows that the Coulomb drag is much stronger than the phonon-mediated drag at physically reasonable $k_F d$. Further, if $2k_F d \sim 1$, the Coulomb drag appears to be much stronger than the phonon-mediated drag, regardless to the temperature. This is the consequence of weakness of the electron-phonon coupling, as compared to Coulomb coupling. However, if $2k_F d$ is large enough, the phonon-mediated drag can overcome the Coulomb drag as the temperature increases, since at $T > s_t/d$ the drag resistance R_D does not contain a small factor of $e^{-4k_F d}$ and increases with T exponentially. Comparing Eq. (33) with Eq. (41), one can find that it occurs when

$$2k_F d > \frac{s_t k_F}{T} + \frac{1}{4}\ln\frac{s_t k_F}{T} + \ln\frac{\pi^{3/4}\rho s_t^2}{3^{1/2}\epsilon h_{14}^2}. \tag{42}$$

The last term in the right-hand side of Eq. (42) is approximately equal to 3.5 for GaAs. Therefore, the phonon-mediated drag can be stronger than the Coulomb drag under

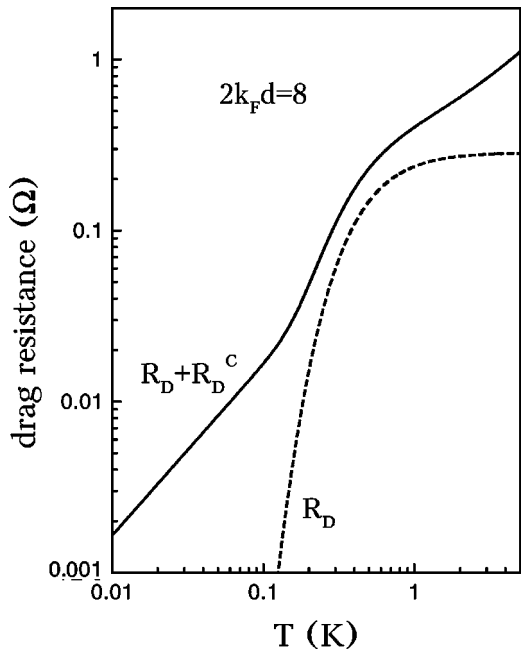

FIG. 6. The temperature dependence of electron drag in GaAs quantum wires of the length $L=2$ μm, width $a=20$ nm and interwire separation $d=200$ nm, at $2k_Fd=8$. The solid line shows the total drag resistance, and the dashed line shows the phonon-mediated drag contribution.

physically reasonable conditions. The phonon-mediated contribution R_D is compared with the total drag resistance $R_D+R_D^C$ in Fig. 6. The calculation of R_D is done by a numerical integration over ω in Eq. (16) using Eqs. (24) and (25) for the matrix elements of the effective interaction, GaAs parameters listed above, and wire parameters $d=200$ nm, $a=20$ nm, and $L=2$ μm, at $2k_Fd=8$. Figure 6 shows that the phonon-mediated drag gives a considerable contribution to the total drag resistance in the region between 0.2 and 2 K. The magnitude of the drag resistance in this region is within the range of experimental measurements. With the increase of $2k_Fd$, the relative contribution of R_D rapidly increases, and at $2k_Fd=10$ the drag resistance in the region above 0.1 K is determined mostly by the phonon-mediated drag contribution. On the other hand, if the factor $2k_Fd$ is smaller than 5, the phonon-mediated drag contribution can be neglected in comparison to the Coulomb drag one.

In conclusion, the description of the electron drag between quantum wires should include consideration of the phonon-mediated interlayer electron-electron interaction if the interlayer distance d is large enough. The behavior of the drag resistance as a function of the temperature and wire parameters depends on whether direct Coulomb drag or phonon-mediated drag prevails. The relative contributions of these two mechanisms can be separated experimentally by measuring the dependence of the drag resistance on the temperature and on the gate voltages controlling 1D electron densities and interlayer distances in the double quantum wire systems.

ACKNOWLEDGMENTS

The author is grateful to Philippe Debray for support and useful discussions.

APPENDIX

The equilibrium one-particle Green's function $G^{(0)-+}$ of Keldysh's technique for fermions of branch j is given by the following expression:

$$G^{(0)-+}_{j\varepsilon}(\mathbf{p})=2\pi i G^{c}_{j\varepsilon}(\mathbf{p})f(\varepsilon), \tag{A1}$$

where $f(\varepsilon)=[e^{(\varepsilon-\mu)/T}+1]^{-1}$ is the Fermi distribution function and $G^c=(G^A-G^R)/2\pi i$ is the causal Green's function, expressed through the retarded (R) and advanced (A) Green's functions. For bosons of branch λ, the equilibrium Green's function $D^{(0)-+}$ is given by

$$D^{(0)-+}_{\lambda\omega}(\mathbf{Q})=-2\pi i D^{c}_{\lambda\omega}(\mathbf{Q})N(\omega), \tag{A2}$$

where $D^c=(D^A-D^R)/2\pi i$, and $N(\omega)=[e^{(\omega-\mu)/T}-1]^{-1}$ is the Planck distribution function. For phonons the chemical potential μ should be set to zero.

The other components of the Green's functions $G^{\alpha\beta}$ are expressed through G^{-+} as

$$\begin{aligned} G^{+-}_{j\varepsilon}(\mathbf{p})&=-2\pi i G^{c}_{j\varepsilon}(\mathbf{p})+G^{-+}_{j\varepsilon}(\mathbf{p}),\\ G^{--}_{j\varepsilon}(\mathbf{p})&=G^{R}_{j\varepsilon}(\mathbf{p})+G^{-+}_{j\varepsilon}(\mathbf{p}),\\ G^{++}_{j\varepsilon}(\mathbf{p})&=-G^{A}_{j\varepsilon}(\mathbf{p})+G^{-+}_{j\varepsilon}(\mathbf{p}), \end{aligned} \tag{A3}$$

and the equations expressing $D^{\alpha\beta}$ through $D^{-+}_{\lambda\omega}(\mathbf{Q})$ are completely analogous to Eq. (A3).

For free electrons with spectrum $\varepsilon_{j\mathbf{p}}$

$$G^{R,A}_{j\varepsilon}(\mathbf{p})=[\varepsilon-\varepsilon_{j\mathbf{p}}\pm i0]^{-1}, \tag{A4}$$

and for free phonons with spectrum $\omega_{\lambda\mathbf{Q}}$

$$D^{R,A}_{\lambda\omega}(\mathbf{Q})=([\omega-\omega_{\lambda\mathbf{Q}}\pm i0]^{-1}-[\omega+\omega_{\lambda\mathbf{Q}}\pm i0]^{-1}). \tag{A5}$$

In Eqs. (A4) and (A5) the upper sign corresponds to the retarded, and the lower sign to the advanced Green's functions.

[1] For a recent review see A. Rojo, J. Phys.: Condens. Matter **11**, R31 (1999).
[2] Yu. M. Sirenko and P. Vasilopoulos, Phys. Rev. B **46**, 1611 (1992).
[3] H.C. Tso and P. Vasilopoulos, Phys. Rev. B **45**, 1333 (1992).
[4] B. Y.-K. Hu and K. Flensberg, *Hot Carriers in Semiconductors*, edited by K. Hess *et al.* (Plenum Press, New York, 1996), p. 261.
[5] B. Tanatar, Phys. Rev. B **58**, 1154 (1998).
[6] V.L. Gurevich, V.B. Pevzner, and E.W. Fenton, J. Phys.: Condens. Matter **10**, 2551 (1998).
[7] O.E. Raichev and P. Vasilopoulos, Phys. Rev. B **61**, 7511 (2000).

[8] V.L. Gurevich and M.I. Muradov, JETP Lett. **71**, 111 (2000).
[9] K. Flensberg, Phys. Rev. Lett. **81**, 184 (1998).
[10] Yu. A. Nazarov and D.V. Averin, Phys. Rev. Lett. **81**, 653 (1998).
[11] R. Klesse and A. Stern, Phys. Rev. B **62**, 16 912 (2000).
[12] V.V. Ponomarenko and D.V. Averin, Phys. Rev. Lett. **85**, 4928 (2000).
[13] P. Debray, P. Vasilopoulos, O. Raichev, R. Perrin, M. Rahman, and W.C. Mitchel, Physica E **6**, 694 (2000).
[14] P. Debray, V. Zverev, O. Raichev, R. Klesse, P. Vasilopoulos, and R.S. Newrock, J. Phys. Condens. Matter **13**, 3389 (2001).
[15] H.C. Tso, P. Vasilopoulos, and F.M. Peeters, Phys. Rev. Lett. **68**, 2516 (1992).
[16] T.G. Gramila, J.P. Eisenstein, A.H. MacDonald, L.N. Pfeiffer, and K.W. West, Phys. Rev. B **47**, 12 957 (1993).
[17] M.C. Bonsager, K. Flensberg, B.Y-K. Hu, and A.H. MacDonald, Phys. Rev. B **57**, 7085 (1998).
[18] S.M. Badalyan and U. Rössler, Phys. Rev. B **59**, 5643 (1999).
[19] H. Noh, S. Zelakiewicz, T.J. Gramila, L.N. Pfeiffer, and K.W. West, Phys. Rev. B **59**, 13 114 (1999).
[20] L.V. Keldysh, Zh. Éksp. Teor. Fiz. **47**, 1515 (1964) [Sov. Phys. JETP **20**, 1018 (1964)]; E.M. Lifshitz and L.P. Pitaevski, *Physical Kinetics* (Pergamon Press, Oxford, 1981).
[21] J.D. Zook, Phys. Rev. **136**, A869 (1964); P.J. Price, Ann. Phys. (N.Y.) **133**, 217 (1981).
[22] O.E. Raichev and P. Vasilopoulos, Phys. Rev. Lett. **83**, 3697 (1999).
[23] J.A. del Alamo and C.C. Eugster, Appl. Phys. Lett. **56**, 78 (1990).
[24] M. Okuda, S.-i. Miyazawa, K. Fujii, and A. Shimizu, Phys. Rev. B **47**, 4103 (1993).
[25] K.J. Thomas, J.T. Nicholls, M.Y. Simmons, W.R. Tribe, A.G. Davies, and M. Pepper, Phys. Rev. B **59**, 12 252 (1999).
[26] T. Ando, A.B. Fowler, and F. Stern, Rev. Mod. Phys. **54**, 437 (1982).
[27] I.S. Gradstein and I.M. Ryzhik, *Tables of Integrals, Series and Products* (Academic, New York, 1980).
[28] The deformation-potential constant in GaAs is not known accurately, and different authors employ values in the range from 7 to 13 eV.